Tellus (1996), 48A, 708–721
Printed in UK – all rights reserved

TELLUS
ISSN 0280–6495

A large-scale horizontal routing model to be coupled to land surface parametrization schemes

By DAG LOHMANN*, RALPH NOLTE-HOLUBE, and EHRHARD RASCHKE *GKSS-Forschungszentrum Geesthacht, Institut für Atmosphärenphysik, Postfach 1160, D-21494 Geesthacht, Germany*

(Manuscript received 17 October 1995; in final form 16 April 1996)

ABSTRACT

The main focus of this paper is the time series analysis of the precipitation-runoff process with transfer functions. Starting from there, a horizontal routing model is constructed to be coupled to the existing land surface parametrization (LSP) schemes which provide the lower boundary conditions in numerical weather prediction and atmospheric general circulation models. As these models currently have a resolution of 10 km–300 km (what we some kind of arbitrary define as the "large scale"), it will be assumed that the horizontal routing process can be lumped as a linear time invariant system. While the main physical properties of the soil (temperature, moisture) and all physical processes (partition of the energy and water fluxes) have to be represented by an LSP scheme, the coupling with a simple routing scheme allows the direct comparison of predicted and measured streamflow data as an integrated quantity and validation tool for both, the atmospheric and the LSP model. The main task of the routing scheme is to preserve the horizontal travel time of water within each grid box as well as from grid box to grid box in the coupled model to first order, while the correct amount of runoff must be given by the LSP scheme. Inverse calculation also allows the direct estimation of runoff which should have been produced by an LSP scheme. As we don't want to deal with snow processes the scheme is applied from February to November.

1. Introduction

In a recent publication of the IAHS "Coupling Large-Scale Hydrological and Atmospheric Models" (Schulz et al., 1995) a number of key problems for meteorologists and hydrologists have been summarized. In currently used numerical weather prediction (NWP) and atmospheric general circulation models (AGCM) the interface between meteorology and hydrology is formed by the land surface parametrization (LSP) schemes. These LSP schemes are now subject to a detailed survey within the GEWEX project PILPS (Henderson-Sellers et al., 1993).

Current LSP schemes in NWP models and AGCMs calculate energy and water fluxes only in the vertical. The driving variables usually include precipitation, wind speed, air temperature, short and longwave radiation, air humidity and pressure. In cases where the latter variables are not available, potential evapotranspiration is estimated using simplified methods (e.g., Shuttleworth, 1993).

LSP schemes have not taken any care of preserving travel time of water in the horizontal direction, because the primary purpose of these models is to partition the downward solar and longwave radiation into sensible, latent and ground heat fluxes and upward longwave radiation, rather than to predict streamflow.

* Corresponding author.
GKSS Research Center, Institute for Atmospheric Physics, PO Box 1160, D-21494 Geesthacht, Germany.
E-mail: lohmann@gkss.de

Todini (1995) states that these water balance (and often also energy balance) LSP schemes characterise the model and constitute the most important part for the coupling of hydrological to atmospheric models. But up to now, the calculated quantity "runoff" (see definition eq. (1)) was not often subject to any further investigation, it essentially vanishes from the water balance of the LSP schemes. The major task of a horizontal routing model coupled to an LSP scheme is to utilize this runoff information to check the reliability of the LSP scheme, giving the opportunity to include streamflow data as an integrated quantity for validation. This also is a question of self consistency of the coupled land–atmosphere model.

LSP schemes using a topographic soil index (Beven and Kirby, 1979; Beven, 1986; Sivaplan et al., 1987) like TOPLATS (Famiglietti and Wood, 1994) can be used to justify more simple LSP schemes. Models with a more detailed physical approach like SHE (Abbott et al., 1986a, b) have a huge parameter space, must be carefully calibrated and are data hungry, facts that often do not correspond to the demands of AGCM and NWP modelers.

The first approaches to include streamflow (Miller et al., 1994; Sausen et al., 1991; Wetzel, 1994; Nijssen et al., 1996; Abdulla, 1995; Abdulla et al., 1996; Russell and Miller, 1990; Kuhl and Miller, 1992; Dümenil and Todini, 1992; and Liston et al., 1994) have used quasi objective or guessed parameters for their horizontal routing schemes. They compared predicted and measured streamflow on a monthly or yearly time step, which seems to us too long for a validation of the processes resolved in the vertical LSP schemes.

In this paper we focus on the construction of a large scale horizontal routing model which can be derived just with measured precipitation and streamflow data on a daily time step. Its derivation involves only a few assumptions about the runoff production process and needs no LSP scheme.

The time scales involved will be examined with the assumption of a linear routing process, which leads us to the well known concept of the unit hydrograph (UH), introduced by Sherman (1932). In the last decade further improvements on this linear concept have been made. In this paper, we will follow the main ideas of the FDTF-ERUHDIT approach ("First Differenced Transfer Function — Excess Rainfall and Unit Hydrograph by a Deconvolution Iterative Technique") (Duband et al., 1993). We will extend it with a simple routine to separate the time scales and couple a linear river routing scheme to it, whichs accounts for the travel time of water in rivers. It solves the linearized Saint-Venant equation (e.g. Mesa and Rifflin, 1986; Fread, 1993) and is optimized with measured streamflow data, although its parameters can also be found with the help of detailed geographic information.

Mathematically the whole model is equivalent to the linear routing model of Wetzel (1994), which was also used in a number of large scale studies (Abdulla, 1995; Abdulla et al., 1996; Lettenmaier, 1995 and references therein) coupled to the LSP VIC-2L model of Liang (Liang, 1994; Liang et al., 1994). Also the scheme of Saussen et al. (1991) can be formulated within this framework.

The German Weser river (see Fig. (1)) has been chosen as the test catchment because of the availablility of long data records of measured precipitation and streamflow. Its catchment above Intschede, the last gauging station not influenced by tides, covers an area of 37495 km^2. Current NWP models and AGCMs have grid lengths of 10 km to 300 km, so that the whole Weser catchment is in the same order of magnitude as one grid box of a AGCM, whereas the smaller catchments of tributaries to the Weser are of the order of one to several NWP model grid boxes. Fig. (1) also shows the grid of the NWP model "Deutschlandmodell" of the German Weather Service (Majewski, 1991; DWD, 1995).

2. The basic idea for the model

Today's LSP schemes which are implemented in AGCMs and NWP models cover a broad range of complexity from a simple bucket model (Manabe, 1969) to more complex schemes. What is common to all of them is that they model the complex nonlinear interactions between the land surface and the atmosphere. In dependence of the soil humidity, soil temperature and the atmospheric boundary conditions they calculate the water and energy fluxes at the land surface. The water balance equation for the terrestrial branch in these LSP schemes may be written as (Peixoto

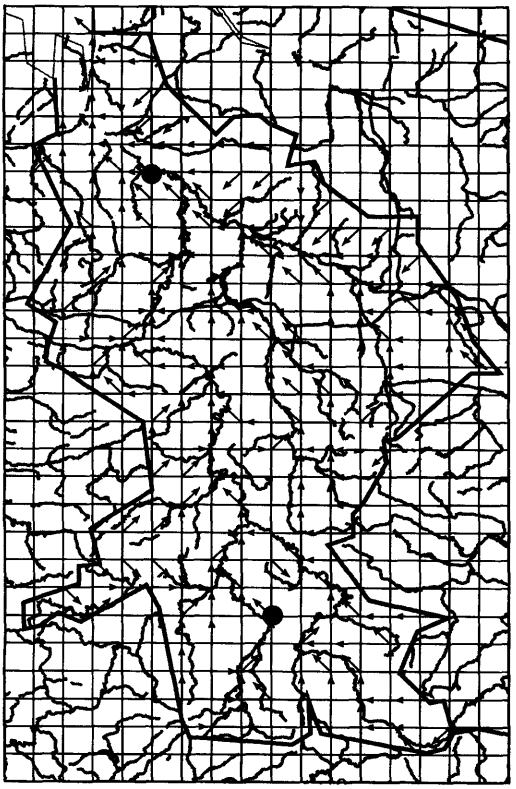

Fig. 1. Weser river catchment flow network with rotated grid 1/8 degree (see DWD, 1995) and gauging stations Intschede (whole Weser) and Rotenburg (subcatchment Fulda). It covers an area of about 37495 km^2 in north central Germany (coordinates: 8–11 E; 50.5–53.5 N).

and Oort, 1992)

$$S = P - E - R_0 - R_U, \tag{1}$$

where S = rate of storage of water, P = precipitation rate, E = evaporation rate, R_0 = surface runoff, R_U = subterranean runoff. R_0 can be seen as a fast component, while R_U reflects the longer time scales. As atmospheric modellers are more interested in the vertical fluxes which feed back to the atmosphere, runoff has not often been subject to any further investigation. As there is an increasing need for water resources management driven by climate and weather prediction models it is important to check the consistency of LSP schemes regarding runoff production. Measured streamflow in rivers is arguably the easiest component of the surface water balance to measure directly, while areal evaporation is very difficult to measure. Arnell (1995) states that "the ability of a climate model to simulate the partitioning of energy at the land surface into latent and sensible heat fluxes can therefore be assessed using observed precipitation and runoff data." In this paper we present a method of how to construct a simple linear routing model for the transformation of runoff from an LSP scheme into streamflow, which afterwards can be compared with measured streamflow.

We are starting from the basic assumptions that all nonlinear processes can be put into a vertical LSP scheme, while the horizontal transfer process from runoff into streamflow is described with a stable causal linear time invariant system. This idea has already been pointed out by various authors (Singh et al., 1982; Littlewood and Jakeman, 1994; Duband et al., 1993; and references therein). The linear transfer function model does lump the horizontal flow properties without being a function of the total soil moisture content itself.

An iterative scheme allows also the inverse calculation, thus giving first hints on what part of the precipitation (called effective precipitation) has to be routed. Cordova and Rodriguez Iturbe (1983) state: ".... the problem is not how to route but what to route". This important feature allows us to compare the calculated effective precipitation with the runoff predicted by an LSP scheme which should be equal.

The theory of linear transfer functions is quite well developed (see Box et al. 1994 and references therein). Given a data series of input $X(t)$ into a linear system and output $Y(t)$ from that system it is in principle straightforward to find a linear transfer function model connecting the two time series. This transfer function model is characterized by its impulse response function (IRF), called unit-hydrograph (UH) by hydrologists.

In a rainfall-streamflow time series analysis this input-output relationship cannot be applied straightforward. On the one hand we do not know the exact input into our system because only a fraction of the precipitation will become streamflow. This process depends strongly on nonlinear processes like soil moisture transport and evapotranspiration. It can be seen as the production part of the overall process represented by an LSP scheme. On the other hand we do not have a transfer function model from an a priori known

input-output relationship. We have two known quantities: precipitation and streamflow. And we have two unknown quantities: the transfer function model and the fraction of the precipitation which becomes streamflow. The main goal of our FDTF-ERUHDIT approach is to find these two unknowns. It provides a balanced treatment for both, the production and the transfer part of the process. Its basic ideas are quite obvious:

- the fraction of precipitation becoming streamflow never exceeds the precipitation itself and is not allowed to become negative
- the IRF is never negative, reflecting that the streamflow is not allowed to decrease because of precipitation
- the routing model is linear, causal, stable and time invariant

These contraints are formulated mathematically in eqs. (2), (10) and (12).

As a starting point, precipitation itself is taken as an approximation of the precipitation becoming streamflow. Of course this is an overestimation and an iterative procedure for the determination of the IRF and effective precipitation will be applied. This iterative part of the model is nonlinear and reflects the nonlinearity of the runoff production process.

A simple river routing scheme will be used to distinguish roughly between the in-grid-box-dynamics and the influence of the river network itself. The linearity of the river routing scheme allows us to deconvolute the IRF from the iterative scheme by the IRF from the river routing scheme. The model's flowchart is schematized in Fig. 2.

Hydrological processes occur at a wide range of time, space, and velocity scales (see Table 1). Within big catchments we normally can't exactly distinguish between the different travel paths the water takes. In this approach all the travel paths we be lumped together in the impulse response function we try to find. It is not clear from first principles that we can find a linear relationship between effective precipitation and streamflow. However, we think that the results strongly encourage this approach.

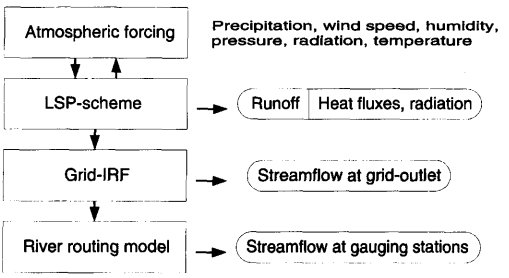

Fig. 2. Coupled LSP scheme and the routing model. One LSP scheme is run for each gridbox, the runoff is then routed to the outlet of that gridbox with an internal impulse response function, and then added to the river routing model which couples all grid boxes together (see also Wetzel (1994)).

3. Method description

3.1. Time scale separation

We are starting from the basic assumption that all horizontal routing processes within a river system (represented by at least one grid box) behave like a causal stable LTI system:

$$Q(t) = \int_0^\infty \mathrm{UH}(\tau) P^{\mathrm{eff}}(t-\tau)\mathrm{d}\tau. \qquad (2)$$

$Q(t)$ is the discharge at a gauging station and $P^{\mathrm{eff}}(t)$ is that part of the precipitation which

Table 1. *Approximate velocity, space and time scales for the different processes involved in horizontal water movement; they only should be seen as a rough estimate, as these processes occur all simultaneously during a precipitation event*

Process/scale	Velocity	Space	Time
rivers	0.5–5 m/s	0–300 km	0–150 h
infiltration excess runoff	10–500 m/h	0–1 km	0–100 h
saturation excess runoff	0.3–100 m/h	0–2 km	0–600 h
ground water	1–10000 m/yr	0–? km	0–years

becomes streamflow. It is always assumed that the precipitation has fallen uniformly over the catchment, which of course does not hold for large catchments and convective precipitation. $UH(t)$ is the impulse response function of the whole system with the condition $\int_0^\infty UH(t)dt=1$.

From the simple scale analysis in Table (1) we can already see that the response to a precipitation event can cover a huge range of time scales. We therefore separate the time scales with the linear model ansatz proposed by Rodriguez (1989) which can be written as a first-order differential equation, representing many simple systems (see Box et al. 1994):

$$\frac{dQ^S(t)}{dt} = -k^*Q^S(t)+b^*Q^F(t), \tag{3}$$

where total flow $Q(t)$=slow flow $Q^S(t)$+fast flow $Q^F(t)$. The explicit solution for $Q^S(t)$ is

$$Q^S(t)=b\int_0^t \exp(-(k+b)(t-\tau))Q(\tau)d\tau \tag{4}$$
$$-Q^S_{(0)}\exp(-(k+b)t),$$

where the initial condition $Q^S_{(0)}$ decays with $\exp(-(k+b)t)$. Eq. (3) is nothing more than a lowpass frequency filter (Press et al., 1992) transforming measured streamflow $Q(t)$ into a fast and a slow component. The parameters k and b are assumed to be constant over the period of calculation. Averaging both sides of eq. (3) in time shows that the fraction of water in the slow component to the water in the fast component is given by

$$\frac{b}{k} = \frac{\text{water in slow flow}}{\text{water in fast flow}}. \tag{5}$$

The parameter k can be estimated using regression analysis of measured $Q(t)$ in periods without or with small fast flow. It determines how fast the linear slow flow storage goes down if there is no or only small input from the fast component. The higher the value of k the smaller is the half time decay $\ln(2)/k$ of the slow flow storage. b can be fitted using the condition $Q(t)-Q^S(t)\geq 0\ \forall t$, as the slow component is never allowed to exceed the total flow. The higher it is the more water is in the slow component. k can also be seen as an effective guiding parameter for the determination of baseflow recession coefficients in LSP schemes using the Arno model conceptualization (Francini and Pacciani, 1991), it already includes all effects of losses due to evapotranspiration.

Assuming that there is an impulse response function $UH^F(t)$ for the fast component, $UH(t)$ can be written as the sum of the impulse response functions for the fast and the slow components

$$UH(t)=UH^F(t)+UH^S(t), \tag{6}$$

which are analytically connected by:

$$UH^S(t)=b\int_0^{t_{max}} UH^F(\tau)\exp(-k(t-\tau)) \tag{7}$$
$$\times\Theta(t-\tau)d\tau.$$

$UH^S(t)$ is an infinite impulse response function with exponential decay, while we assume that $UH^F(t)$ is a finite impulse response function with a maximal length t_{max}. The step function Θ is given by $\Theta(t)=0$ for $t<0$ and $\Theta(t)=1$ for $t\geq 0$. With $UH^S(t)$ from eq. (7) we already have a solution of eq. (3). As eq. (2) is a linear superposition of solutions with given amplitudes $P^{eff}(t)$ we have found the solution of eq. (2) if we can find $UH^F(t)$ and $P^{eff}(t)$.

3.2. *Estimation of the fast impulse response function and the effective precipitation*

Having selected the two parameters of the slow flow model from measured data, we can compute $UH^F(t)$ and $P^{eff}(t)$ with the following procedure (as described by the first part of Fig. (3)):

- make slow flow separation with the slow flow model, eq. (3);
- solve iterative scheme with minimal least-squares solution, starting with P^{eff}_i=precipitation at time instant i in eq. (9).

If there are n data points of precipitation and if $(m-1)^*$ timestep is the assumed length t_{max} of the fast flow impulse response function, the equation

$$Q^F(t)=\int_0^{t_{max}} UH^F(\tau)P^{eff}(t-\tau)d\tau \tag{8}$$

can be written for the discrete case as

$$\begin{pmatrix} Q^F_m \\ \vdots \\ Q^F_n \end{pmatrix} = \begin{pmatrix} P^{eff}_m & \cdots & P^{eff}_1 \\ \vdots & \ddots & \vdots \\ P^{eff}_n & \cdots & P^{eff}_{n-m+1} \end{pmatrix} \tag{9}$$
$$\times\begin{pmatrix} UH^F_0 \\ \vdots \\ UH^F_{m-1} \end{pmatrix}$$

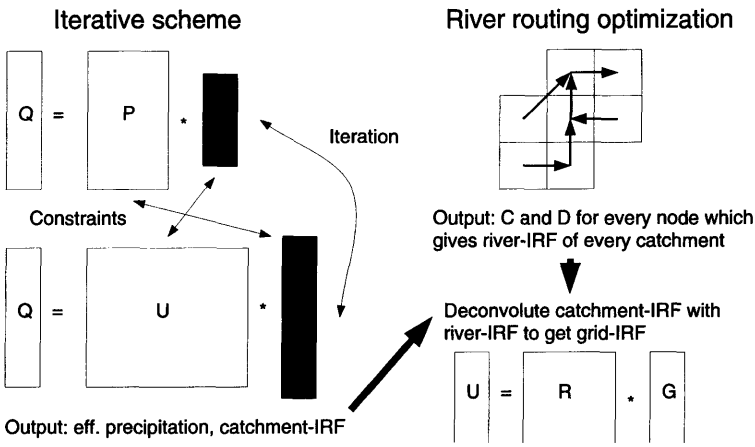

Fig. 3. Flowchart of the two-component routing scheme. The iterative scheme is solved via eqs. (9) and (11). The river routing is optimized with least-squares. Afterwards the impulse response function (IRF) of the iterative scheme is deconvoluted with the IRF of the river network. Q = fast flow, P = precipitation, U = fast flow IRF, R = river-IRF, G = grid-IRF.

for the calculation of $\mathrm{UH}_i^{\mathrm{F}}$. In the discrete case UH^{F} already includes the timestep Δt. After every calculation we apply the constraint

$$\sum_{i=0}^{m-1} \mathrm{UH}_i^{\mathrm{F}} = \frac{1}{1+b/k} \text{ with } \mathrm{UH}_i^{\mathrm{F}} \geqslant 0 \,\forall\, i, \tag{10}$$

which follows from the fixed fraction of the water in the fast and slow component, the fact that $\int_0^\infty \mathrm{UH}(t)\mathrm{d}t = 1$ and the non-negativeness of $\mathrm{UH}(t)$. UH^{F} is then put into the matrix of (11) and the following equation is solved for P^{eff}:

$$\begin{pmatrix} Q_m^{\mathrm{F}} \\ \vdots \\ \vdots \\ Q_n^{\mathrm{F}} \end{pmatrix} = \begin{pmatrix} \mathrm{UH}_{m-1}^{\mathrm{F}} & \dots & \mathrm{UH}_0^{\mathrm{F}} & 0 & \dots & 0 \\ 0 & \ddots & \ddots & \ddots & \ddots & \vdots \\ \vdots & \ddots & \ddots & \ddots & \ddots & 0 \\ 0 & \dots & 0 & \mathrm{UH}_{m-1}^{\mathrm{F}} & \dots & \mathrm{UH}_0^{\mathrm{F}} \end{pmatrix} \times \begin{pmatrix} P_1^{\mathrm{eff}} \\ \vdots \\ \vdots \\ P_n^{\mathrm{eff}} \end{pmatrix}. \tag{11}$$

Again, after every iteration, the constraint

$$0 \leqslant P_i^{\mathrm{eff}} \leqslant \text{precipitation}_i \,\forall\, i \tag{12}$$

is applied to P_i^{eff}, which afterwards is put into eq. (9) for the next iteration.

The difference to the method reviewed in (Duband et al., 1993) is, that we are not using several single precipitation events, but long data series of precipitation and streamflow. This is necessary due to the strong varying baseflow component and the overlapping of precipitation events. Furthermore we are not calculating the differenced transfer function, but the transfer function directly. The solution of eqs. (9) and (11) is obtained with a minimal least-squares solution using the F04JAF and F04JDF routines of the NAG Fortran Library, Mark 16 (1993). For a review of solution techniques of the equations see also (Singh et al., 1982; Duband et al., 1993).

3.3. *Limitations of the model*

From the model design itself we can already discover some of the model limitations. The first one is that it is build as a LTI system with homogeneous precipitation. But without that assumption we would rarely get a transfer function of the system. The next large limitation is the fixed fraction of fast flow to the slow flow. During snow melt processes a much higher fraction of the melt

water will go into the fast component, so that the model reloads the slow component too much. But unless the model is coupled to an LSP and snow-melt scheme, it will not be able to deal with snow and ice processes, because than we would need to know the snow melt time series. In all calculations with a fixed fraction the results have been reasonably good.

The coefficients k and b, as the UH^F itself, must be seen as lumped parameters, as the surface is often quite heterogeneous on the scale of 10 to 300 km. UH^F reflects a three dimensional water transport process, while it is only one dimensional. This is also interesting for the LSP schemes. We can't say from first principles, how fast in which depth of an LSP scheme the horizontal routing processes occur. The distinction of fast and slow horizontal processes in large scale LSP schemes has to be made scaleable and must be calibrated with measured data.

One important point is, that $n/2$ should always be much larger than m. Otherwise we can't say that we have found a parsimony transfer function model. If $n/2 \approx m$, the algebraic system in the eqs. (9) and (11) becomes quadratic and can always approximately be solved. This also stresses the important point of a slow flow separation. The correlation length between precipitation and streamflow would otherwise be too long in the case of a finite impulse response function, which means, m would be too large.

Like already pointed out by Duband et al. (1993) there has been no proof that the solutions are unique, nor that they are physically sound rather than a purely numerical artefact. Finally the assumptions made in the model can only be justified by the results. In subsection (5.2), we show the convergence of the impulse response function in 3 to 5 iteration steps.

4. River routing

River routing within the model is done with the linearized Saint-Venant equation (Mesa and Mifflin, 1986; Fread, 1993). We constructed an approximate river network with the resolution of the atmospheric model from maps and digitized data. The arrows in Fig. (1) reflect the main flow directions of the natural streams. While the in-grid-dynamic of the horizontal routing process is described with a transfer function model, we transport the water coming out of a grid box through other grid boxes with a simple linear river routing model. This way of thinking implicitly assumes that water is not transported out of a grid box with processes other than river flow.

In the linearized Saint-Venant equation

$$\frac{\partial Q}{\partial t} = D \frac{\partial^2 Q}{\partial x^2} - C \frac{\partial Q}{\partial x}, \tag{13}$$

the parameters C and D can be found from measurements or by rough estimation from geographical data of the riverbed. Wave velocity C and diffusivity D must be seen as effective parameters, as there is often more than one river in a grid box or because of human-made changes. Finally we end up with one C and one D value for every grid box, which reflect the main characteristics of the water transport in a river.

Eq. (13) can be solved with convolution integrals

$$Q(x, t) = \int_0^t U(t-s)h(x, s)\mathrm{d}s, \tag{14}$$

where

$$h(x, t) = \frac{x}{2t\sqrt{\pi t D}} \exp\left(-\frac{(Ct-x)^2}{4Dt}\right) \tag{15}$$

is the Green's function (or impulse response function) of eq. (13) with boundary values and initial condition $h(x, 0) = 0$ for $x > 0$ and $h(0, t) = \delta(t)$ for $t \geqslant 0$. Due to its linearity and the numerical stability of this solution scheme the influence of dams, weirs and wateruse can easily be implemented into the scheme at every node. The solution with convolution integrals also avoids difficulties when the parabolic eq. (13) tends to become more hyperbolic in character for $P = L^*C/D > 100$, where P is the dimensionless Peclet number and L the distance between two neighboring grid points. A large P reflects the fact that river runoff is basically an advection rather than a diffusion process. This approach uses the ideas by Todini (1991) without the inclusion of backwater effects and with constant velocities.

5. Calculations and results

5.1. *Data for the calculations*

Calculations have been carried out for the whole Weser catchment above Intschede (an area of

37,495 km^2), and for subcatchments of tributaries. Results will be shown for the whole Weser and for the Fulda catchment above Rotenburg (2523 km^2) for February to November 1993 (303 days).

The data we used for the calculation are the operational daily precipitation data from the German Weather Service (DWD) and river discharge data from the German Federal Institute of Hydrology (BfG) and the Niedersächsisches Landesamt für Ökologie (NLfÖ). 10 years of daily precipitation data of more than 300 stations and ten years of daily averaged river discharge data of 38 selected gauging stations had been available.

5.2. *The slow flow separation and the iterative scheme*

The required time t_{max} for the fast flow component can be seen from the simple time scale analysis. After a time of approximately 600 hours, all fast processes should have decayed. For all calculations we took $m=24$ or $t_{max}=23$ days, which seemed to be a reasonable value for all fast processes together, higher values like $m=32$ or $m=48$ have not changed the results, leading basically to noise in the tail of the IRF. Lower values of m simply cutoff the IRF. We have $279=303-24$ equations for determining UH^F while we only have 23 free parameters (the 24 samples of UH^F and one condition from eq. (10). So we can argue: if there is a reasonable impulse response function for the fast component which is able to explain the shapes of the flood waves in the river then the routing system is linear to a very good approximation.

Figs. 4, 5 show the slow flow separation at the gauging stations Rotenburg and Intschede. From measured data (b, k) were chosen to be (0.017, 0.0169) for Rotenburg and (0.038, 0.0173) for Intschede in units of [1/day]. This already shows that the Weser river is dominated by the slow component in eq. (3). The values of b and k are not unambiguous, although they can't be varied in a large range (up to 30%). However, we think that they finally must be calibrated together with an LSP scheme which is also able to distinguish between fast and slow components in the runoff production process. As shown in eq. (4) the initial condition of $Q^S(0)$ decays with $\exp -(k+b)t$, so its amplitude is halved after 12 to 20 days.

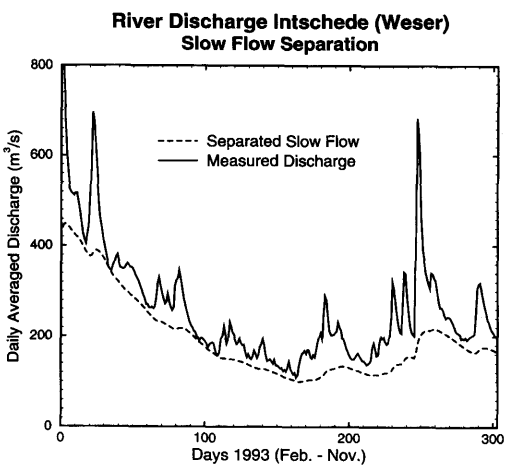

Fig. 4. Slow flow separation for the Fulda river at Rotenburg. $b=0.017$/day, $k=0.0169$/day.

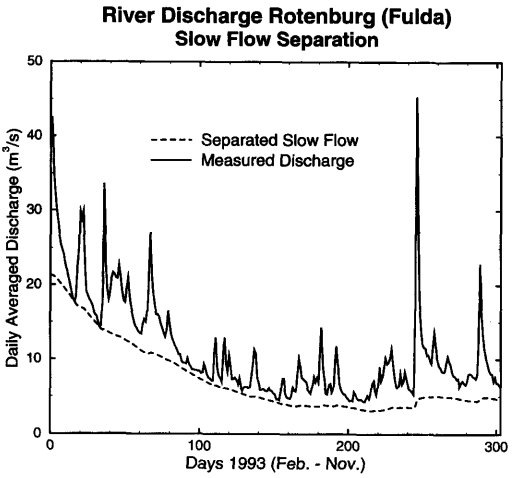

Fig. 5. Slow flow separation for the Weser river at Intschede. $b=0.038$/day, $k=0.0173$/day.

The first answer to the question of the quality of the chosen linear model comes from the model results. After 3–5 iterations, the results remain nearly unchanged during further iterations, so the scheme becomes stable. Fig. 6 shows the fast IRF of the catchment above Rotenburg from the first 5 iterations. The IRFs from the iterative scheme are shown in Figs. 7, 8. The peak times from Rotenburg and Intschede show only a one day difference. The reason for that seems to be spatially correlated precipitation, especially in autumn, where evapotranspiration is low and the floods

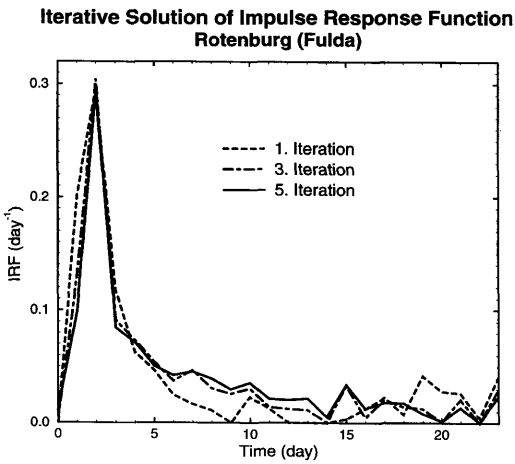

Fig. 6. Impulse response functions of the iterative scheme. Shown are the impulse response functions of the first, third and fifth iteration for Rotenburg (Fulda).

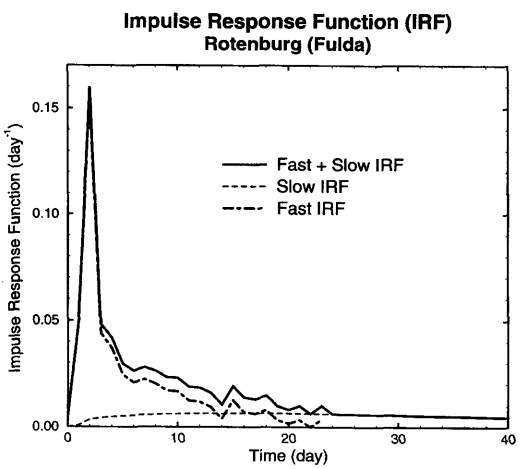

Fig. 7. Impulse response function for the Fulda catchment above Rotenburg. Shown are the fast, the slow and the sum of both impulse response functions.

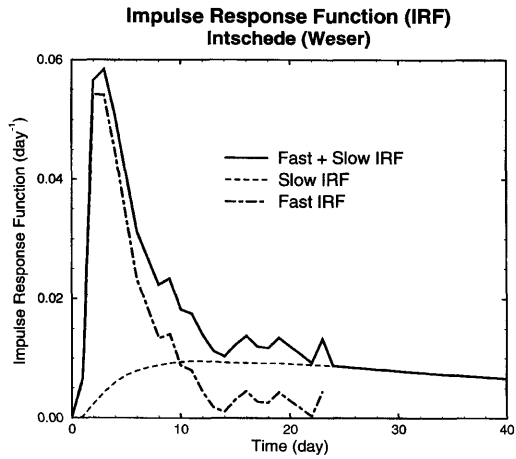

Fig. 8. Impulse reponse function for the whole Weser catchment above Intschede. Shown are the fast, the slow and the sum of both impulse response functions.

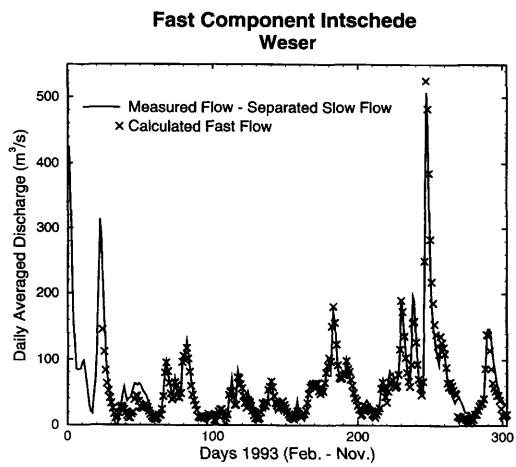

Fig. 9. Time series of the measured flow minus the separated slow flow versus the iteratively calculated fast flow from Rotenburg (Fulda).

are becoming higher. As the eqs. (9) and (11) are solved with a minimal least-square solution, the scheme adapts to these precipitation events. Also the water wave in the Weser river only needs approximately 2 days to go from Rotenburg to Intschede.

Figs. 9, 10 show the results of the fast flow component as a time series, whereas the scatterplots, Figs. 11 and 12, show the general performance of the model. The iterative scheme had problems at the beginning of March due to snow melt processes, which can't be resolved by the model without a coupling to a snow-melt model. The deconvoluted effective precipitation can be expected to be a good approximation for the runoff which should have been produced by an LSP scheme within an error of 1 or 2 days, which seems to be the approximate uncertainty by this simple approach for the fast component. Regarding the slow component we must be very careful with the interpretation of the results. The

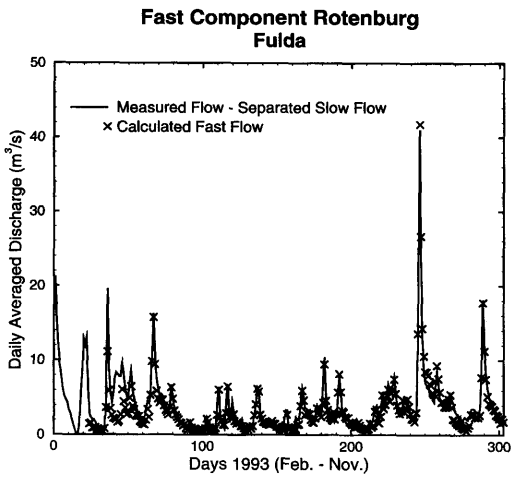

Fig. 10. Time series of the measured flow minus the separated slow flow versus the iteratively calculated fast flow from Intschede (Weser).

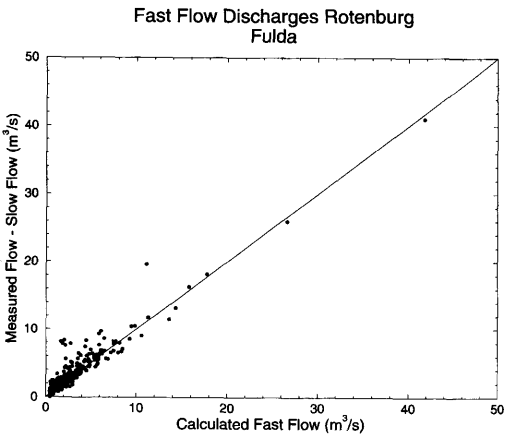

Fig. 11. Scatter-plot of the measured flow minus the separated slow flow versus the iteratively calculated fast flow from Rotenburg (Fulda).

parameters b and k vary in nature dependent on the soil moisture status, and the simple time scale separation does not include real soil moisture processes. We can only investigate these problems with a coupling to an LSP scheme which explicitly resolves the vertical moisture fluxes and parametrizes the baseflow. However, in the derivation of the iterative scheme it was important to separate the time scales, otherwise the correlation length between the river discharge and the precipitation would have been too long (the half life time of the

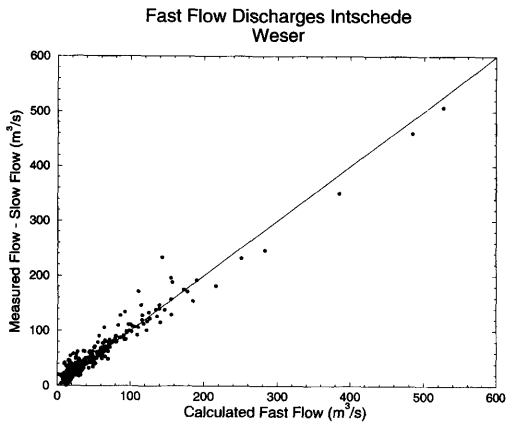

Fig. 12. Scatter-plot of the measured flow minus the separated slow flow versus the iteratively calculated fast flow from Intschede (Weser).

exponential slow flow storage decay is approximately 40 days). It thus only can give us a first hint on how baseflow recession curves in large scale LSP schemes have to look like. It gives us a rough idea of how the soil effectively memorizes a precipitation event in the first weeks.

Because this approach is catchment based rather than grid based, there of course always remains the problem of how to adress the deconvoluted effective precipitation if there are different contributing grid boxes. As one of our basic assumptions was that the precipitation has fallen uniformly over the catchment we can only assign proportional fractions to each grid cell in the catchment.

5.3. *Optimized river routing*

First, the effective parameters C and D between neighbouring gauging stations for a 1 year period of hourly interpolated streamflow data have been optimized with a least-square solution. That means we were looking for an optimal river impulse response function $h(x, t)$ from eq. (15) between two gauging stations. C and D were then checked over a long time period, typically 3 years. C and D values upstream from the last gauging station were assumed to be the same as the downstream value from that gauging station.

Velocities C are normally in the range of 1 to 3 m/s and diffusivities are about 200 to 4000 m^2/s. The optimization procedure finally will give constant C and D values for every single gridbox for

all further calculations with the routing scheme. Holding the parameters C and D constant can be justified by assuming large errors in the other model parts. In the full Saint-Venant equations (Fread, 1993) the flow velocity depends on the amount of water which is transported. Because LSP schemes are quite inacurate regarding runoff production and atmospheric models do not necessarily provide the right amount of precipitation, a nonlinear model would be more sensitive to these model errors. So we use a linear model because of practical reasons. This is also a question on what time scale finally a comparison of measured and modelled data should be done.

Fig. 13 shows the total river network impulse response function. We supplied the river grid network with a one hour input at each grid node. The whole response function reflects the time the river network needs to transport water to the last gauging station in Intschede. From there we already can conclude that the river network has a stronge influence on the time to peak in the impulse response function (Fig. 8) from the iterative scheme, which includes all different processes. The distinction between river routing and other processes can approximately be done as is shown in subsection (5.4).

One problem that will always occur in large scale hydrology is the incorporation of human-made changes in nature, specially weirs, dams and artificial lakes. As this optimization is already done to today's streamflow data, it can be expected to give an approximate picture of the horizontal routing process in rivers. The detailed inclusion of dams and lakes normally requires accurate dam and lake managing data and procedures, if their effects can't be described by an increase of D and a decrease of C and by simple storage threshold routines.

5.4. *Grid box IRF*

In regions where no river discharge data are available for most of the grid boxes, we still can find an average grid box IRF for the catchment. It can be derived for each single grid box by deconvoluting the IRF from the iterative scheme by the IRF from the linear river routing optimization for that catchment. This can be done with Toeplitz matrizes or more advanced solution techniques (Press et al., 1992). Therefore one river-IRF is calculated for every catchment, as shown in Fig. 13 for the whole Weser river. For deconvolution the river-IRF is summed up to daily values. The lumped gridboxes all have the same internal IRF afterwards. Fig. 14 shows such a deconvoluted IRF for the whole Weser catchment above Intschede. The deconvoluted grid-IRF tells us how horizontal water transports in the average grid

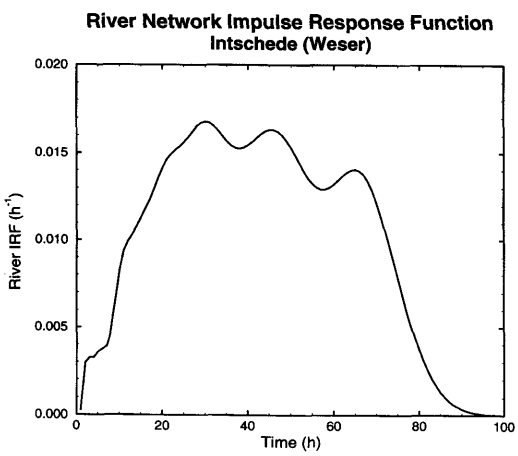

Fig. 13. River-impulse response function for the whole Weser catchment above Intschede. Input has been a one hour water supply at every grid node of the optimized river routing scheme.

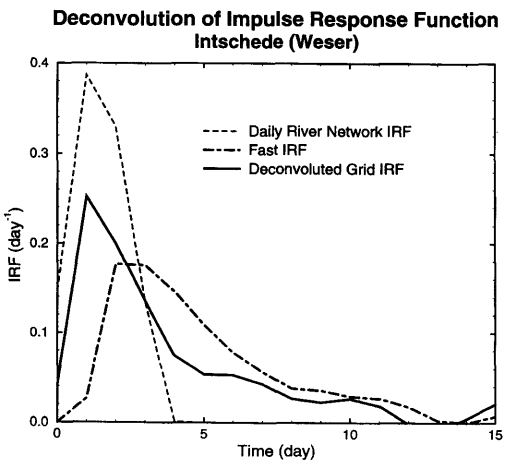

Fig. 14. Deconvoluted impulse response function of the iterative scheme with the river-impulse response function of the catchment network for the whole Weser River. Output is a uniform grid-impulse response function for every grid box in the catchment.

box within the catchment occur. In nature of course there will not be the same IRF for every gridbox. But as NWP models are now resolving a finer grid than operational hydrological measurements are available, we have to deal with an average grid IRF to distinguish between river routing and internal grid-IRF. This approach is similar to (Mesa and Mifflin, 1986), although we used an optimized river network IRF with non homogeneous C and D for the deconvolution. We also had not to look for a width function of the river, as this function is already given by the river network itself and we even did not use a width function for every single grid box.

As this approach comes from the empirical side and thus already includes all effects of human-made changes in nature, the authors assume that it will be difficult to justify a more detailed model on this scale which should be coupled to current LSP models on the large scale. A possible step forward would be to allow the IRF to vary with total soil moisture within each grid box, as it is recommended by Todini (Todini 1995). In fact, the coupling of this horizontal routing scheme to an LSP model already means that the fraction of water in the fast component to the water in the slow component can vary, dependent on the soil moisture, the parametrization of the vertical water transport processes and the assumptions about the baseflow recession curve.

The idea of how to couple the model finally to an LSP scheme is simple. Some of today's LSP schemes (Wood et al., 1992; Liang et al., 1994; Dümenil and Todini, 1992) have implemented simple parameterizations regarding their baseflow processes (e.g., the Arno-model (Francini and Pacciani, 1991)). These are build as linear storage models, some have a threshold where the storage–outflow relationship becomes nonlinear. The baseflow component can approximately be identified with the slow component in eq. (3), although the time constants will vary due to evaotranspiration losses in the LSP scheme. This baseflow component together with a fast component, e.g., from a variable infiltration capacity equation and other infiltration equations (W. J. Rawls et al., 1993; and references therein) will then be convoluted with the deconvoluted grid box fast impulse response function before they are put into the river routing model.

6. Conclusions

The coupling of some easy-to-use and to understand tools can form a powerfull basis for a first order approximation of nature. We do not claim originality as parts of the constructed model have been used elsewhere before. However, we think that this simple model exactly fullfils the demands which LSP modellers have right now, especially on the scale of todays NWP models. Derived from measured data, the constructed routing model is the simplest model to preserve the lumped horizontal travel time of water when coupled to an LSP scheme. Due to (a) human-made changes for wateruse, (b) the absence of a detailed global hydrological data set even in near future and (c) large errors in other model components of coupled models (e.g., precipitation), more physically based (and sometimes even overparameterized) models on the current scale of AGCMs and NWP models are difficult to justify. Although simple, an LSP scheme coupled to this routing model represents a closed model for the description of water and energy fluxes in the hydrosphere. While the physics of the whole model is in the LSP scheme, this routing model allows to include measured streamflow data as a verification tool in the coupled atmospheric-hydrological model.

One of the main advantages of this simple approach is the inverse calculation of effective precipitation (or runoff) which might lead to a better understanding of the processes resolved in vertical LSP schemes. It can be doubted whether the assumption of constant velocities and diffusivities, which are actually reflected by the shape of the IRF of the iterative scheme and its first and second moments, does hold in extreme cases like snowmelt processes or very dry conditions. This has to be checked together with an LSP scheme. But, the overall concept would allow the IRF to change its form and the parameters b and k to differ for different snow and soil moisture situations. Then one iteration process has to be done for each of those situations.

Using a model based on convolution integrals is not very appropiate in atmospheric models, as they provide prognostic and diagnostic variables only for up to four time levels. So, in near future we will use simple parameterizations for the impulse response functions. We will do regionalisation studies (see also Littlewood and Jakeman,

1994), as we need for this approach good precipitation and streamflow data, which are not available for most of the globe. The model right now is used as a postprocessor for daily runoff data.

In near future coupled model runs will be performed together with the VIC-2L model from Liang [Liang 1994] in BALTEX and GCIP catchments.

Finally, it is hoped that a justification of the model within its errors can be done with a more physically based hydrological model with grid lengths of less than 1 km on the catchment scale of about 100 to 10,000 km^2.

7. Acknowledgements

The authors want to thank the German Weather Service (DWD) for providing us with precipitation data, the German Federal Institute of Hydrology (BfG) and the Niedersächsisches Landesamt für Ökologie (NLfÖ) for providing us with streamflow data. The corresponding author wants to thank the German Academic Exchange Service (DAAD) for financial scholarship support (DAAD-Doktorandenstipendium aus Mitteln des zweiten Hochschulsonderprogramms) during his visit at the University of Washington (USA) and Prof. Dennis P. Lettenmaier for hosting him. The second author acknowledges support by the German Ministry of Science and Education, BMBF, grant 07 VWK 01/6. We also wish to thank Ute Karstens, Manfred Lobmeyr and Burkhardt Rockel from the GKSS BALTEX-group for inspiring discussions.

REFERENCES

Abbott, M. B., Bathurst, J. C., Cunge, J. A., O'Connell, P. E. and Rasmussen, J. 1986a. An introduction to the European Hydrological System — Système Hydrologique Européen, "SHE", 1: History and philosophy of a physically-based, distributed modelling system. *J. Hydrol.* **87**, 45–59.

Abbott, M. B., Bathurst, J. C., Cunge, J. A., O'Connell, P. E. and Rasmussen, J. 1986b. An introduction to the European Hydrological System— Système Hydrologique Européen, "SHE", 2: Structure of a physically-based, distributed modelling system. *J. Hydrol.* **87**, 61–77.

Abdulla, F. A. 1995. *Regionalization of a macroscale hydrological model.* Dissertation, Department of Civil Engineering, University of Washington, USA.

Abdulla, F. A., Lettenmaier, D. P., Wood, E. F. and Smith, J. 1996. Application of a macroscale hydrologic model to estimate the water balance of the Arkansas-Red River basin. *J. Geophys. Res.* **101**, 7449–7459.

Arnell, N. W. 1995. River runoff data for the validation of climate simulation models. In: Springer NATO ASI Series, vol. 131, H. R. Oliver and S. A. Oliver (eds.), *The Role of Water and the Hydrological Cycle in Global Change*, 349–371.

Beven, K. 1986. Runoff production and flood frequency in catchments of order *n*: an alternative approach. In: V. K. Gupta, I. Rodriguez-Iturbe and E. F.Wood (eds.), *Scale Problems in Hydrology*, pp. 107–131.

Beven, K. J. and Kirby, M. J. 1979. A physically based, variable contributing area model of basin hydrology. *Hydrol. Sci. Bull.* **24**, 43–69.

Blöschl, G. and Sivaplan, M. K. 1995. Scale issues in hydrological modelling: a review. In: J. D. Kalma and M. Sivapalan (eds.), *Advances in hydrological processes*, 9–48.

Box, G. E. P., Jenkins, G. M. and Reinsel, G. C. 1994. *Time series analysis, forecasting and control*, 3rd edition. Prentice Hall, Englewood Cliffs, New Jersey.

Cordova, J. R. and Rodriguez-Iturbe, I. 1983. Geomorphologic estimation of extreme flow probabilities. *J. Hydrol.* **65**, 159–173.

Duband, D., Obled, Ch. and Rodriguez, J. Y. 1993. Unit hydrograph revisited: an alternate iterative approach to UH and effective precipitation identification. *J. Hydrol.* **150**, 115–149.

Dümenil, L. and Todini, E. 1992. A rainfall-runoff scheme for use in the Hamburg climate model. In: *Advances in theoretical hydrology, A tribute to James Dooge*, J. P. O'Kane (ed.). European Geophysical Society Series on Hydrological Sciences 1, Elsevier, Amsterdam, pp. 129–157.

DWD, 1995. *Dokumentation des EM/DM-Systems.* Abteilung Forschung, Deutscher Wetterdienst, Zentralamt, Offenbach am Main.

Famiglietti, J. S. and Wood, E. F. 1994. Multiscale modeling of spatially variable water and energy balance processes. *Water Resour. Res.* **30**, 3061–3078.

Francini, M. and Pacciani, M. 1991. Comperative analysis of several conceptual rainfall-runoff models. *J. Hydrol.* **122**, 161–219.

Fread, D. L. 1993. Flow routing. In: *Handbook of hydrology*, ch. 10. D. R. Maidment (ed.). McGraw Hill.

Henderson-Sellers, A., Yang, Z.-L. and Dickinson, R. E. 1993. The project of intercomparison of land-surface parametrization schemes. *Bull. Amer. Meteor. Soc.* **74**, 1335–1349.

Kuhl, S. C. and Miller, J. R. 1992. Seasonal river runoff calculated from a global atmospheric model. *Wat. Resour. Res.* **28**, 2029–2039.

Lettenmaier, Dennis P. 1995. Modeling of runoff and streamflow at regional to global scales. In: Sprigner NATO ASI Series Vol. 131 H. R. Oliver and S. A. Oliver (eds.). *The role of water and the hydrological cycle in global change*, pp. 297–316.

Liang, X. 1994. *A two-layer variable infiltration capacity land surface representation for general circulation models.* Water Resources Series Technical report no. 140. Department of Civil Engineering, University of Washington.

Liang, X., Lettenmaier, D. P., Wood, E. F. and Burges, S. J. 1994. A simple hydrologically based model of land surface water and energy fluxes for general circulation models. *J. Geophys. Res.* **99**(D3), 14415–14428.

Liston, G. E., Sud, Y. C. and Wood, E. F. 1994. Evaluating GCM land surface hydrology parameterizations by computing discharges using a runoff routing model: application to the Mississippi basin. *J. Appl. Met.* **33**, 394–405.

Littlewood, I. G. and Jakeman, A. J. 1994. A new method of rainfall-runoff modelling and its application in catchment hydrology. In: *Environmental modeling*, vol. **II**, P. Zannetti (ed.). Computational Mechanics Publications, pp. 143–171.

Majewski, D., 1991. The Europamodell of the Deutscher Wetterdienst. ECMWF course: *Numerical methods in atmospheric models*, vol. **2**, pp. 147–191.

Manabe, S. 1969. Climate and the ocean circulation 1. The atmospheric circulation and the hydrology of the Earth surface. *Mon. Weather Rev.* **97**, 739–774.

Mesa, O. J. and Mifflin, E. R. 1986. On the relative role of hillslope and network geometry in hydrologic response. In: V. K. Gupta, I. Rodriguez-Iturbe and E. F. Wood (eds.). *Scale Problems in Hydrology*, pp. 1–17.

Miller, J. R., Russell, G. L. and Caliri, G. 1994. Continental-scale river flow in climate models. *J. Climate* **7**, 914–28.

NAG, 1993. *The NAG Fortran Library Manual*, Mark **16**, The Numerical Algorithms Group Limited.

Nijssen, B., Lettenmaier, D. P., Liang Xu, Wetzel, S. W. and Wood, E. F. 1996. Streamflow simulation for continental-scale river basins. *J. Geophys. Res.*, submitted.

Peixoto, J. P. and Oort, A. H., 1992. *Physics of climate.* American Institute of Physics.

Press, W. H., Teukolsky, S. A., Vetterling, W. T. and Flannery, B. P. 1992. *Numerical Recipes in Fortran.* Cambridge Press.

Rawls, W. J., Ahuja, L. R., Brakensiek, D. L. and Shirmohammadi, A. 1993. Infiltration and soil water movement. In: *Handbook of hydrology*, chapter 5, D. R. Maidment (ed.). McGraw Hill.

Rodriguez, J. Y. 1989. *Modélisation pluie-débit par la méthode DPFT.* Thése de doctorat, Grenoble, France.

Russell, G. L. and Miller, J. R., 1990. Global river runoff calculated from a global general circulation model. *J. Hydrol.* **116**, 241–254.

Saussen, R., Schubert, S. and Dümenil, L. 1991. *A model of river-runoff for use in coupled atmosphere-ocean models; large-scale atmospheric modelling.* Report no. 9, Meteorologisches Institut der Universität Hamburg, FRG.

Schulz, G. A., Hornbogen, M., Viterbo, P. and Noilhan, J. 1995. *Coupling large-scale hydrological and atmospheric models.* IAHS Special Publications no. 3.

Sherman, L. K. 1932. Streamflow from rainfall by the unit hydrograph method. *Eng. News. Rec.*, 108.

Shuttleworth, W. J. 1993. Evaporation. In: *Handbook of hydrology*, ch. 4, D. R. Maidment (ed.). McGraw Hill.

Singh V. P., Baniukiewicz, A. and Ram, R. S. 1982. Some empirical models of determining the unit hydrograph. In: *Rainfall-runoff relationship*, V. P. Singh (ed.): Water Resources Publications, pp. 67–90.

Sivaplan, M. K., Beven, K. and Wood, E. F. 1987. On hydrologic similarity, 2, A scaled model of storm runoff production. *Water Resour. Res.* **23**, 2266–2278.

Todini, E. 1991. Hydraulic and hydrologic flood routing schemes. In: NATO ASI Series C: vol. 345. D. S. Bowles and P. E. O'Connell (eds.). *Recent Advances in the Modeling of Hydrologic Systems*, pp. 389–406.

Todini, E. 1995. New trends in modelling soil processes from hillslope to GCM scales. In: Springer NATO ASI Series, vol. 131. H. R. Oliver and S. A. Oliver (eds.), *The role of water and the hydrological cycle in global change*, pp. 317–347.

Wetzel, S. 1994. A hydrological model for predicting the effects of climate change. B.S. Thesis, Princeton University, Department of Civil Engineering and Operations Research.

Wood, E. F., Lettenmaier, D. P. and Zartarian, V. G. 1992. A land-surface hydrology parameterization with subgrid variability for general circulation models. *J. Geophys. Res.* **97**, 2717–2728.